

Observation of Radiative Capture in Relativistic Heavy-Ion-Atom Collisions

R. Anholt, S. A. Andriamonje,^(a) E. Morenzoni,^(b) Ch. Stoller, J. D. Molitoris, and W. E. Meyerhof
Department of Physics, Stanford University, Stanford, California 94305

and

H. Bowman, J.-S. Xu,^(c) Z.-Z. Xu,^(c) and J. O. Rasmussen
*Nuclear Sciences Division, Lawrence Berkeley Laboratory,
 University of California, Berkeley, California 94720*

and

D. H. H. Hoffmann
Gesellschaft für Schwerionenforschung, Darmstadt, West Germany
 (Received 9 April 1984)

X-ray studies of relativistic heavy-ion-atom collisions allow the direct observation of the radiative-electron-capture photons. The angular distribution of these photons is approximately $\sin^2\theta_{\text{lab}}$, because of the cancellation of electron retardation effects when the cross sections are subjected to Lorentz transformation into the laboratory frame. Comparison of measured and calculated cross sections reveals the number of equilibrium projectile K vacancies present in the solid targets, which can be compared with charge-state measurements behind the target.

PACS numbers: 34.50.Hc

The charge state of an ion traveling through a solid target is governed by the cross sections for loss (ionization) and capture of electrons.¹ Radiative and nonradiative electron capture are possible. For nonradiative capture, the electron makes a transition from a target orbital to a projectile orbital, and the difference in electron binding energy is converted to projectile kinetic energy. For radiative capture (REC) of target electrons into the projectile K shell, which is dominant in collisions of heavy projectiles on light target atoms, the electron loses energy, which is converted into electromagnetic energy. The availability of relativistic heavy ions at the Lawrence Berkeley Laboratory Bevalac allows the direct observation of the radiative part of the capture cross section by observing the photon. Since capture into the projectile K shell requires the presence of projectile K vacancies, the number of REC photons seen in sufficiently thick targets is proportional to the number of equilibrium K vacancies, giving a direct measure of this quantity *inside the target*. Comparison is possible in some of the present cases with charge-state measurements behind the target.^{2,3}

Measurements of cross sections for target K -vacancy production, projectile K x-ray production, and REC were made. Further experimental details will be presented in a forthcoming publication.⁴ The cross sections were normalized by counting each projectile impinging on the target (with a peak counting rate of approximately 10^4 Hz). The tar-

gets used were of equilibrium thickness; also, the projectile was stripped to its equilibrium charge state in an upstream Si transmission particle detector.

Figure 1 shows an x-ray spectrum taken with an intrinsic Ge x-ray detector in 197-MeV/u Xe + Be collisions. The most prominent feature in this (logarithmic) spectrum is the K REC peak at approximately 125 keV. The REC peak energy E_{peak} in the projectile frame is the sum of the electron kinetic energy, $(\gamma - 1)mc^2$, where $\gamma^{-2} = 1 - \beta^2$, $\beta = v/c$, and v is the ion velocity, and the K electron binding energy E_K , which has approximately the value given by the one-electron Dirac equation.⁵ In the laboratory, this energy is Doppler shifted according to

$$E_{\text{REC}} = E_{\text{peak}} \gamma^{-1} (1 - \beta \cos\theta_{\text{lab}})^{-1} \quad (1)$$

where θ_{lab} is the angle between the beam axis and the photon direction. The width is determined mostly by the angular opening $\Delta\theta_{\text{lab}}$ of the x-ray detector.

Also seen in Fig. 1 is a shoulder at lower x-ray energies, composed of REC into the projectile L and M shells and a primary bremsstrahlung continuum.⁶ Primary bremsstrahlung (or radiative ionization) is the radiative scattering of target electrons from the projectile nucleus. The spectrum has an end point in the projectile frame given by the electron kinetic energy $(\gamma - 1)mc^2$, and in the laboratory frame by an equation similar to Eq. (1).⁴ Also

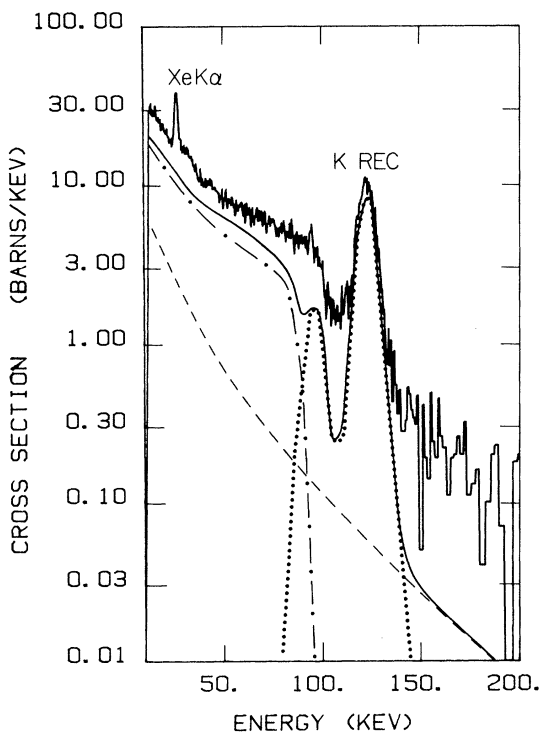


FIG. 1. Spectrum of photons detected at $\theta_{\text{lab}}=90^\circ$ in 197-MeV/u Xe + Be collisions. Calculated (Ref. 4) contributions from K and L REC (dotted line), SEB (dashed line), and primary bremsstrahlung (chain line) are shown.

present in this spectrum are Xe projectile K x rays and secondary-electron bremsstrahlung (SEB). In collisions with target atoms of $Z_T \geq 50$, observation of REC is not possible, because SEB, which increases quadratically with Z_T , dominates over the linearly varying REC and primary bremsstrahlung. At present the discrepancies between the bremsstrahlung calculations and experiment are incompletely understood, as will be discussed in a forthcoming paper.⁴

Figure 2 shows the angular distribution of K REC photons for 197-MeV/u Xe + Be collisions. In the projectile frame, REC is the inverse photoeffect. An electron impinges on a projectile ion, and the angular distribution of the emitted photon including electron retardation effects is of the form^{5,7}

$$d\sigma/d\Omega \sim \sin^2\theta/(1 - \beta\cos\theta)^4, \quad (2)$$

which is peaked in the projectile frame in the direction opposite the beam direction. If this distribution is subjected to Lorentz transformation into the laboratory frame, which folds the backward-peaked angular distribution forward, one obtains an angular distribution varying as $\sin^2\theta_{\text{lab}}$.⁷ Equation (2) is

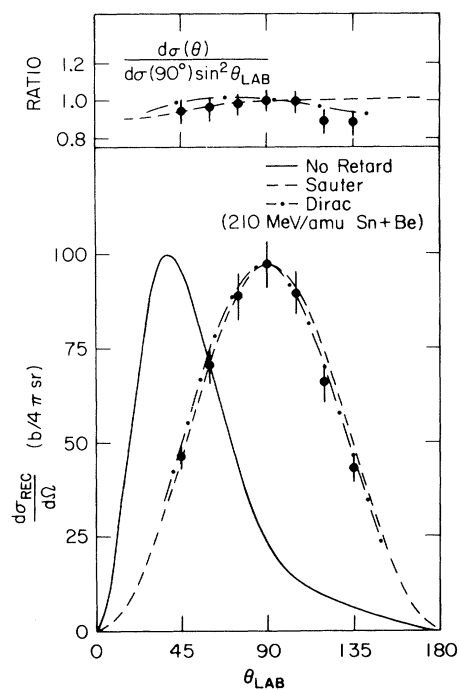


FIG. 2. Angular distribution of K REC photons in 197-MeV/u Xe + Be collisions and the ratio to $\sin^2\theta_{\text{lab}}$ normalized at $\theta_{\text{lab}}=90^\circ$. Dashed line: plane-wave Born calculations of Sauter (Ref. 8); chain curve calculated with Dirac wave functions (Ref. 9) for 150-keV photons incident on Sn, hence appropriate for similar 210-MeV/u Sn + Be collisions. Solid curve: no retardation included in the photoelectric cross section.

only approximate for relativistic electrons incident on high- Z ions. Calculations of photoelectric angular distributions by Sauter⁸ and Hultberg, Nagel, and Olsson⁹ give deviations from $\sin^2\theta_{\text{lab}}$ smaller than $\pm 10\%$. The latter⁹ Dirac calculations are most appropriate here since the high- Z projectiles are nearly fully stripped. The data agree better with the Dirac calculations, though the $\pm 6\%$ experimental uncertainties do not preclude either calculation.

Figure 3 compares our measured and calculated integrated REC cross sections. Where counting statistics are negligible, the absolute uncertainty in the photon cross sections is approximately $\pm 12\%$.⁴ As Z_T increases, the cross sections become increasingly uncertain, because of the uncertainty in the background subtraction of SEB. In the impulse approximation⁷, the K REC cross section is the Dirac K -shell photoelectric cross section for the projectile atom⁹ multiplied by phase-space factors:

$$\sigma_{K \text{ REC}} = Z_T \left(\frac{E_{\text{peak}}}{\gamma\beta mc^2} \right)^2 \sigma_{K \text{ PE}}(E_{\text{peak}}), \quad (3)$$

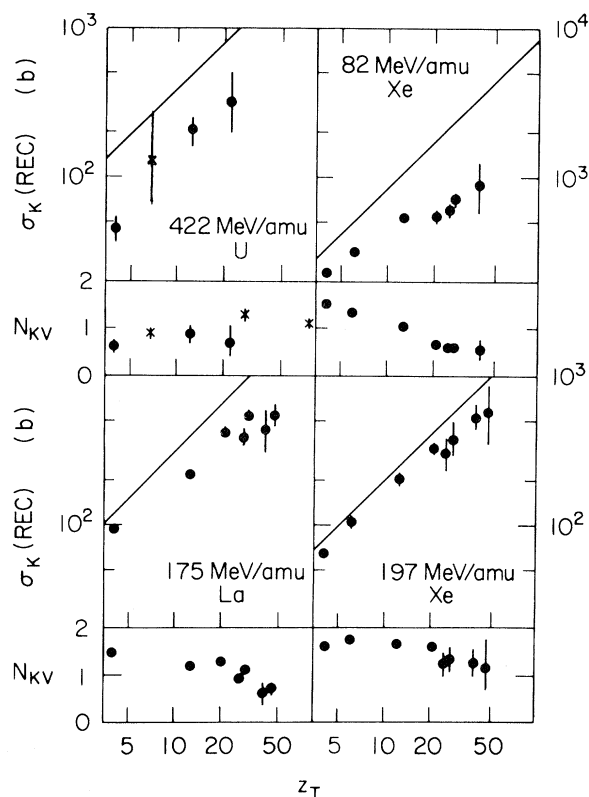


FIG. 3. Measured and calculated K REC cross sections and the deduced average number of projectile K vacancies. Crosses are from post-target charge-fraction measurements of Gould *et al.* (Ref. 2) for 437-MeV/u ^{238}U ions for Mylar ($Z_T = 6.6$), Cu, and Ta targets.

where Z_T is the number of available target electrons per atom. The photoelectric cross section is per projectile atom, and hence the REC cross section is for a fully stripped projectile ion. The difference between the higher calculated REC cross sections, σ_{calc} , and the measured ones, σ_{meas} , in Fig. 3 indicates that fewer than two projectile K vacancies are present inside the target. The number of K vacancies can be calculated from

$$N_{Kv} = 2\sigma_{\text{meas}}/\sigma_{\text{calc}}. \quad (4)$$

The projectile charge state is determined by a competition between electron loss and capture. Electron loss by ionization is expected to increase as Z_T^2 . At low Z_T , where REC dominates, capture is proportional to Z_T [Eq. (3)], but at high Z_T , where nonradiative capture dominates, capture is proportional to some high power of Z_T , such as $Z_T^{5.10}$. Hence N_{Kv} is expected to increase with Z_T at low Z_T and decrease at a higher Z_T values, depending on when nonradiative capture dominates over ionization. This general trend is apparent in Fig. 3.

For the U projectile data, one can compare our findings for N_{Kv} within the target with the 437-MeV/u U charge-state determination of Gould *et al.*² behind the target, the difference in projectile energies being negligible. Calling the corresponding K -vacancy number N'_{Kv} , one has

$$N'_{Kv} = 2F_0 + F_1, \quad (5)$$

where F_0 and F_1 are the charge fractions for zero and one electron, respectively. The values of N'_{Kv} are shown by crosses in Fig. 3.

With high- Z , highly stripped ions such as 422-MeV/u U, one does not expect any long-lived metastable states to be formed inside the target, which then possibly autoionize upon leaving the target, giving higher post-target vacancy fractions.³ Within the experimental uncertainties, nearly equal in-target and post-target vacancy fractions are found, in agreement with this expectation. The exceptional U+Ti N_{Kv} point is least certain, because of the difficulty of separating the REC peak from the SEB background.

Gould *et al.*² extracted capture cross sections for U from the target-thickness dependence of the charge fractions. These cross sections should be compared with the calculated capture cross section into all shells of the fully stripped projectile. In Fig. 3, the solid lines indicate σ_{calc} for REC into the fully stripped K shell. If all other shells are included, the cross section is approximately 30% higher. For 437-MeV/u U + Mylar ($Z_T = 6.6$), the experimental cross section² does not agree well with theory. Capture cross sections are more difficult to extract from charge-state measurements than from x-ray measurements, as reflected by the larger error bars.

The determination of the K -vacancy number in solid targets rests on the accuracy of the calculated REC cross sections. A recent formulation¹¹ of the strong Born approximation for REC suggests that the K REC cross sections should be a factor of 4 to 6 higher than the impulse-approximation results. The use of this theory would produce much smaller vacancy fractions (by a factor of $\frac{1}{6}$ to $\frac{1}{4}$ in U), in severe disagreement with the charge-fraction measurements. A recalculation of the strong-Born REC cross section is in closer agreement with the impulse-approximation results.¹²

Until now, x-ray and magnetic charge-state analysis studies in heavy-ion-atom collisions have not been well coordinated. The x-ray and charge-state measurements complement one another and provide additional information on the charge state of ions inside and behind solid targets.

This work was supported in part by the National

Science Foundation Grant No. PHY-83-13676, in part by the Department of Energy contract No. DE-AC-03-76-SF00098, and in part by the Swiss National Fond, and for one of us (G.A.A.) by a NATO postdoctoral fellowship. Discussions with E. Spindler, D. H. Jakubassa-Amundsen, F. Bell, and H. D. Betz are greatly appreciated. K. Baker, D. Spooner, D. Murphy, K. Frankel, K. Crowe, and W. McHarris took part in some of the data taking.

(a)Permanent address: Centre d'Etudes Nucléaires, University of Bordeaux, Gradignan, France.

(b)Present address: Laboratory for Medium-Energy Physics, Eidgenössische Technische Hochschule Hönggerberg, Zurich, Switzerland.

(c)Permanent address: Department of Physics, Fudan University, Shanghai, Peoples Republic of China.

¹H. D. Betz, *Rev. Mod. Phys.* **44**, 465 (1972).

²H. Gould, D. Greiner, P. Lindstrom, T. J. M. Symons, and H. Crawford, *Phys. Rev. Lett.* **52**, 180 (1984).

³H. D. Betz and L. Grodzins, *Phys. Rev. Lett.* **25**, 211 (1970).

⁴R. Anholt, S. A. Andriamonje, E. Morenzoni, Ch. Stoller, J. D. Molitoris, W. E. Meyerhof, H. Bowman, J.-S. Xu, Z.-Z. Xu, J. O. Rasmussen, K. Frankel, D. Murphy, K. Crowe, and D. H. H. Hoffmann, to be published.

⁵H. A. Bethe and E. E. Salpeter, *Quantum Mechanics of One- and Two-Electron Atoms* (Academic, New York, 1957).

⁶H. W. Schnopper, J. P. Delvaille, K. Kalata, A. R. Sohval, M. Abdulwahab, K. W. Jones, and H. E. Wegner, *Phys. Lett.* **47A**, 61 (1974).

⁷E. Spindler, H. D. Betz, and F. Bell, *Phys. Rev. Lett.* **42**, 832 (1979).

⁸F. Sauter, *Ann. Phys. (Leipzig)* **9**, 217 (1931) and **11**, 454 (1931).

⁹S. Hultberg, B. Nagel, and P. Olsson, *Ark. Fys.* **38**, 1 (1967).

¹⁰G. Raisbeck and F. Yiou, *Phys. Rev. Lett.* **4**, 1858 (1971).

¹¹M. Gorriz, J. S. Briggs, and S. Alston, *J. Phys. B* **16**, L665 (1983).

¹²D. H. Jakubassa-Amundsen, R. Höppler, and H. D. Betz, to be published.